

Introduction

The Vera C. Rubin Observatory's LSST Camera (LSSTCam) uses an instrument signature removal (ISR) algorithm to generate defect masks for its CCDs. We compare the defect mask generated by ISR from flat images from test runs 6 (06/22/2023) and 6b (11/16/2023), and verify the ISR defect algorithm performance. We find a mischaracterization of the edge region of the detectors, with different behavior for different detectors.

The current defect masking algorithm classifies these regions as dark defects and contaminates the defect set at the >90% level, preventing a study of the dark defects and any evolution of them between different data-collection runs. We performed a study of the edge regions and the mid-line bloom to measure excluded pixel regions. To define these excluded regions, we use deviations from flatness along the entire detector.

Reclassifying these picture-frame artifacts as a different mask type will allow a precise examination of the dark defects in the focal plane, and any changes between different data-collection runs.

Defect Masks

The present defect masking algorithm flags any pixel above or below 20% of the median of a flat image as a bright or dark defect, respectively.

We find differences in the defect mask's counts for the two runs, including notably elevated dark defect counts.

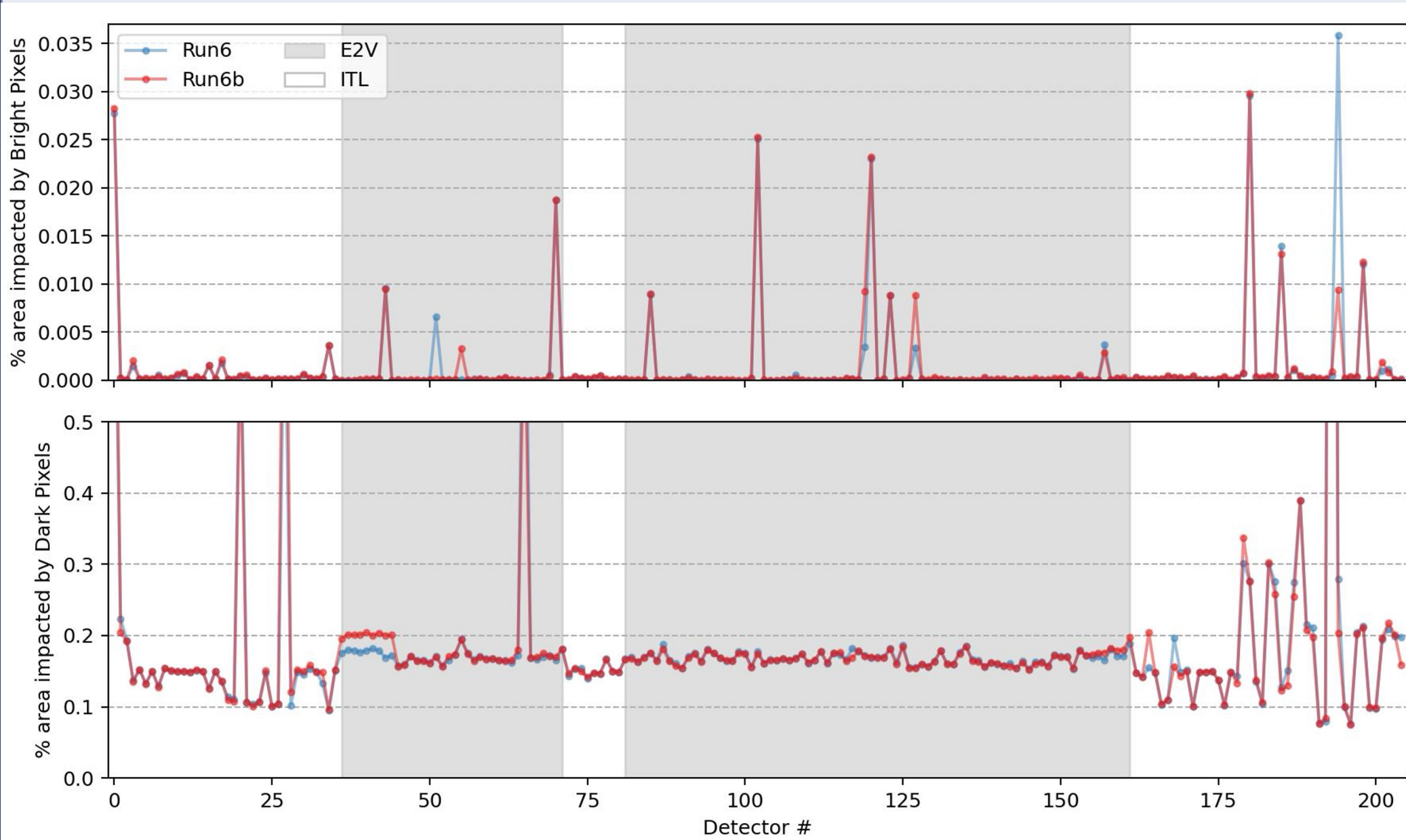


Fig. 1: Upper panel: The area of bright defects for each detector in both Run 6 (22/06/2023) and Run 6b (16/11/2023), with shaded regions showing the different detector types. Lower panel: Plot of the area of bright defects for each detector in both Run 6 and Run 6b, with shaded regions showing the different detector types.

		Bright median [%]	Dark median [%]
Run 6	ITL	2.118E-04	1.489E-01
	E2V	5.488E-05	1.685E-01
Run 6b	ITL	2.425E-04	1.490E-01
	E2V	7.317E-05	1.688E-01

Table 1: Statistics from Fig. 1 of the median area for different detectors

Picture-Frame Masking

The most striking feature from Fig. 1 is the elevated baseline dark defect level compared to bright defects. The dark defects also are at different levels for different detector types, varying by ~0.02%.

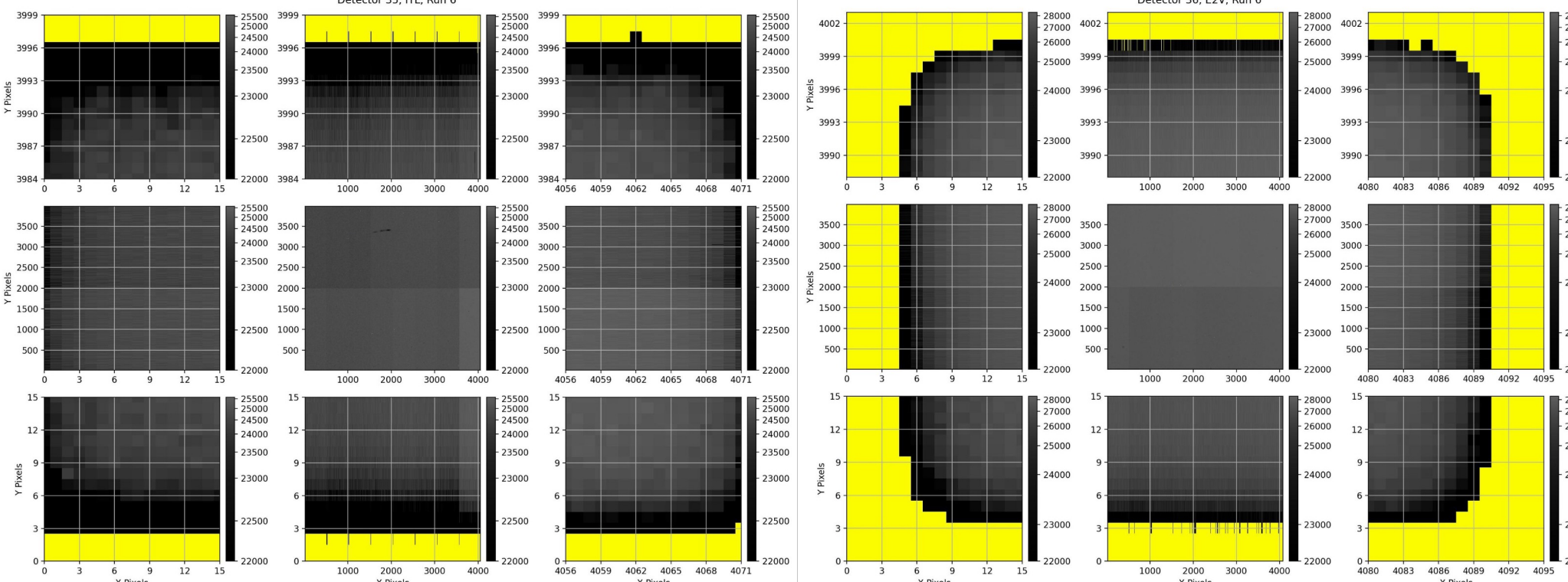


Fig. 2: Flat images of ITL and E2V sensors, with dark defect masks in yellow.

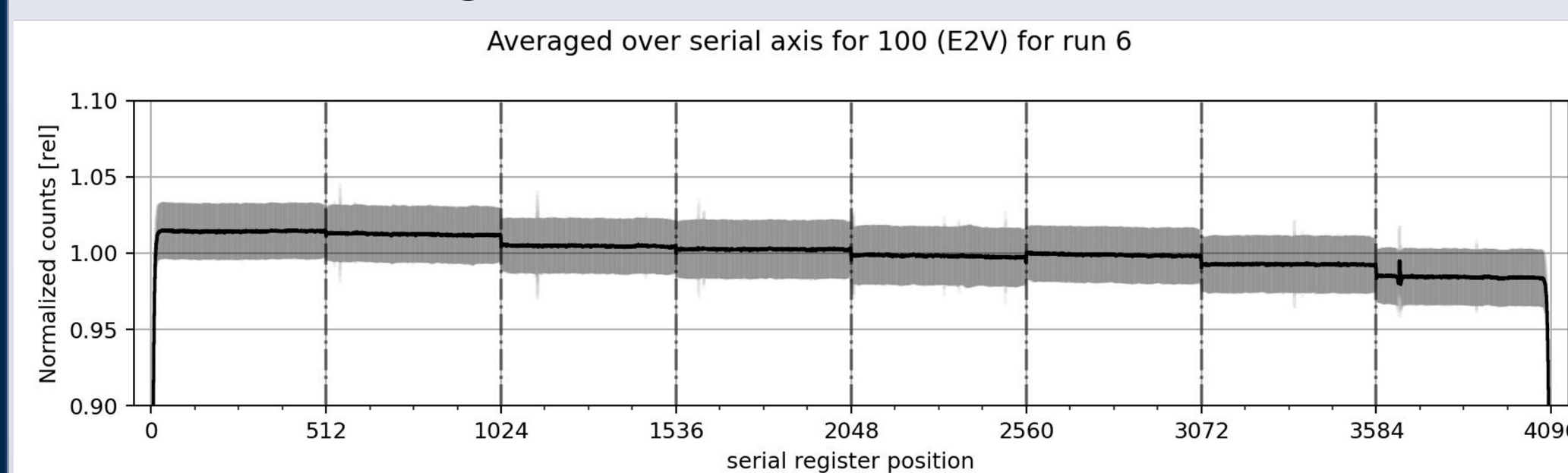
The elevated baseline level of the dark defects in both data collection runs motivated the examination of the edges of the detectors and masking in that region. The edges of these detectors in Fig. 2 show dark defects for both types of detectors.

Is this a problem? A Brief Calculation

- Typical edge defects for ITL detectors ~6 pixels across edge of detector → 6/4000 ~ 1.5E-01% area
- Typical dark median was 1.5-1.7E-01%
- A large proportion (if not all) of the currently characterized dark defects are edge defects! We cannot study the defects without properly treating the edges

Detector Grouping and Flattening

To measure the level of masking required for the pictureframe, we collect flats from detectors of the same type - E2V, ITL, and ITL corner. For each type of detector, the post-ISR flat images from a test run are normalized to the median value of the individual detector, along either the serial and parallel axes. This gives a measure of the relative difference along these axes due to the pictureframe edge, or the mid-line bloom.



Combine data from all similar detectors

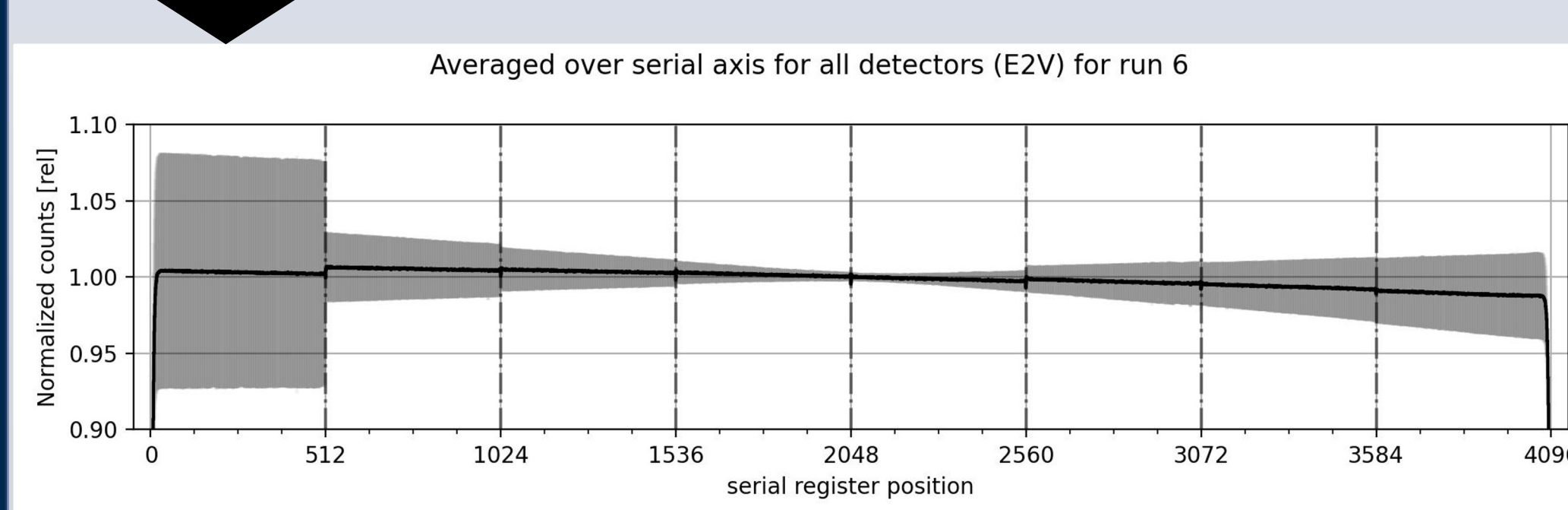


Fig. 3: Method for combining flats of the same detector type, and binning along either serial or parallel axes

Edge Roll-Off region

To define exclusion of picture-frame pixels, we normalize the measurement of a single detector type binned along a specific axis to a 'normalizing region', and count the pixels that deviate from the median of the 'normalizing region.'

For the serial axis, the 'normalizing' region was defined as the adjacent amplifier. For the parallel axis, it was defined as the area of the detector up to the mid-line bloom.

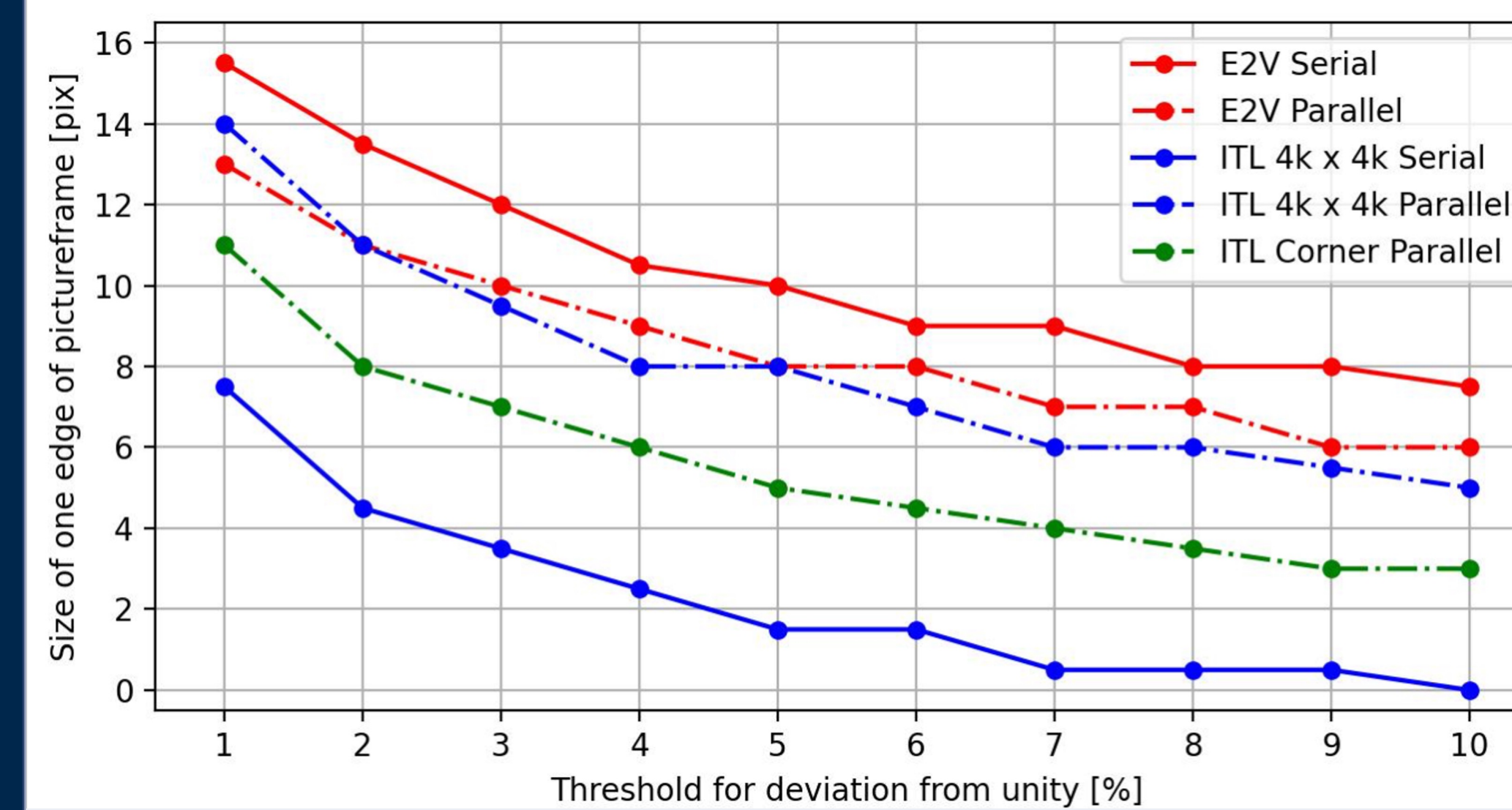


Fig. 4: Pixel edge exclusion size along detector edges, varied as a function of different deviation thresholds. Common detector types are plotted in the same color, and common axes are plotted with the same linestyle

Mid-Line Bloom

In addition to decreased response at the detector edges, the detectors experience a non-linear response at the mid-line blooming feature.

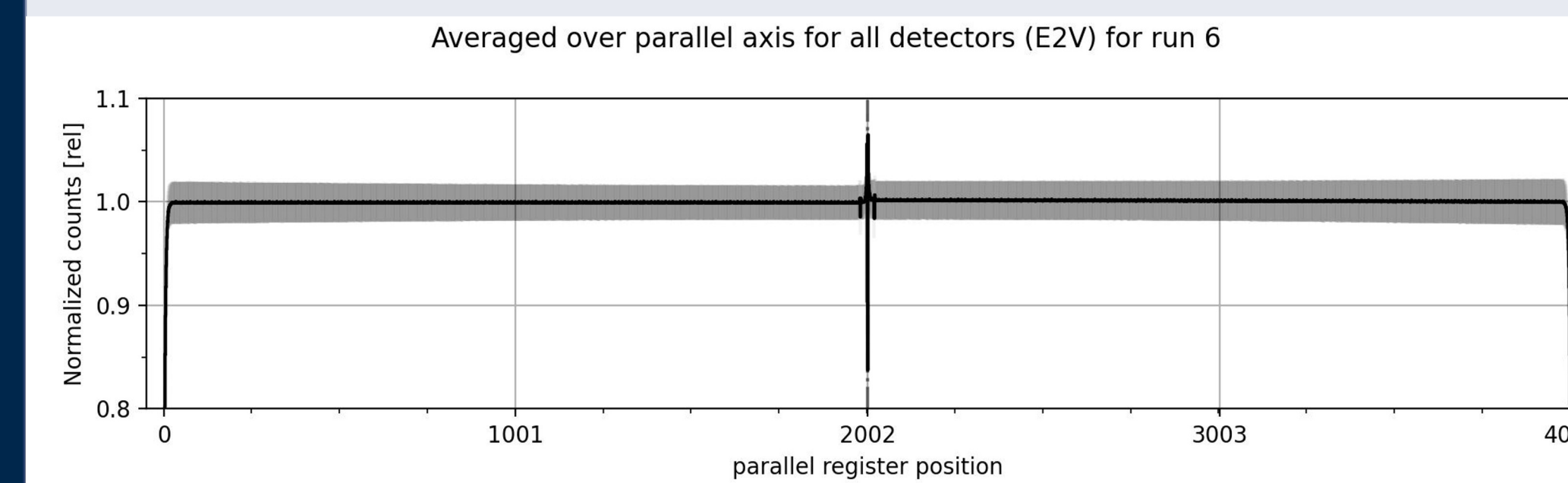


Fig. 5: Intensity values of all E2V detectors averaged along the parallel register

To define exclusion of mid-line pixels, we apply the same methodology as before with the normalizing region instead being the whole detector.

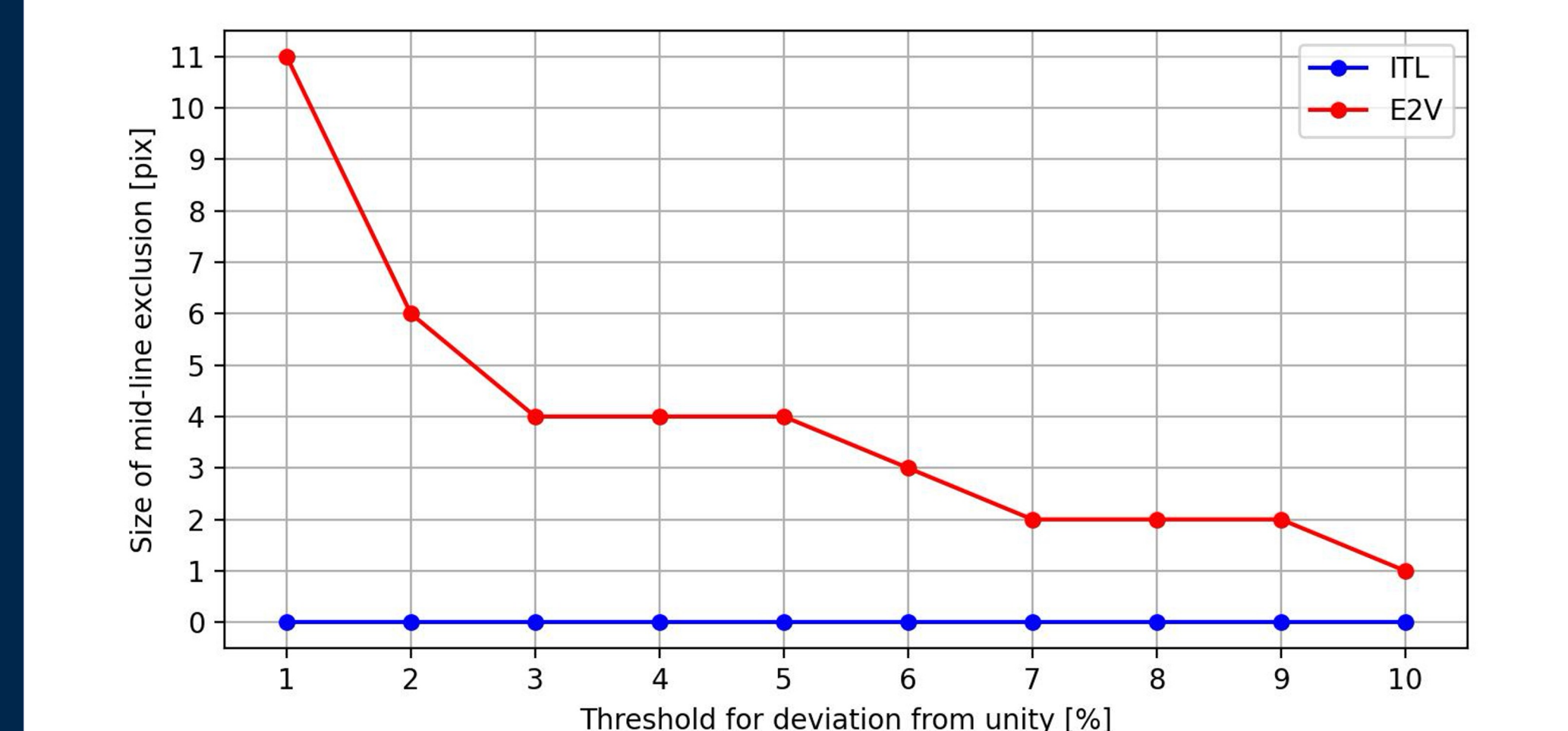


Fig. 6: Pixel edge exclusion size at mid-line bloom, varied as a function of different deviation thresholds.

Results

The edge region of the ITL detector is dominant in the parallel axis and has weak edge sensor effects along the serial axis. In comparison, the E2V detectors show an edge region that is dominant in the serial axis and has moderate edge sensor effects in the parallel axis.

The midline bloom region differs significantly between the two types of detectors. E2V detectors show a large fluctuation along the midline bloom, while the ITL detectors have a weak fluctuation, <1% deviation from flatness when using the combined flat images.

Conclusions

We have characterized response along detector edges and the mid-line bloom for different detector types. Using the methods described, we can develop a preliminary estimate of the masking size as a function of flatness deviation thresholds.

With these thresholds and the corresponding pixel exclusions, we can use the focal plane fill-factor verification report (LCA-19636-A) that defines focal plane active area to compare the thresholds to previously reported detector features and connect them to ISR.

	Edge Roll-off		Mid-line bloom	
	FP fill report	Corresponding threshold	FP fill report	Corresponding threshold
ITL	9 pixels	2%	N/A	N/A
E2V	9 pixels	5%	5 pixels	2-3%

Table 2: Pixel edge exclusion thresholds, corresponding to sensor edge response roll-off and mid-line bloom size at mid-line bloom, varied as a function of different deviation thresholds.

This study successfully verifies the lack of a mid-line blooming feature in the ITL detectors and provides a direct recommendation to ISR for defining picture-frame and mid-line bloom features.

Once this ISR picture-frame mask is implemented, we will begin a detailed study of bright and dark defects and their evolution between data collection runs.

These results serve as the platform for an additional study of individual detector-level thresholds to further meet the values from the focal plane fill-factor verification report. In this study, vignetting of the beam and its effect on the edge response will also be examined.

Acknowledgments

This work is supported by the National Science Foundation AST-1910719. This work is supported in part by the National Science Foundation through Cooperative Agreement AST-1258333 and Cooperative Support Agreement AST1836783 managed by the Association of Universities for Research in Astronomy (AURA), and the Department of Energy under Contract No. DE-AC02-76SF00515 with the SLAC National Accelerator Laboratory managed by Stanford University.